Magnetic properties of Fe - Cr-based nanocrystalline alloys

1997 J. Phys.: Condens. Matter 9 10485

(http://iopscience.iop.org/0953-8984/9/47/016)

J. Phys.: Condens. Matter **9** (1997) 10485–10500. Printed in the UK PII: S0953-8984(97)82938-4

Magnetic properties of Fe–Cr-based nanocrystalline alloys

N Randrianantoandro†, A Ślawska-Waniewska‡ and J M Greneche†

† Laboratoire de Physique de l'Etat Condensé, URESA CNRS 6087, Université du Maine, F72085 Le Mans Cédex 9, France

‡ Institute of Physics, Polish Academy of Sciences, Aleja Lotników 32/46, 02-668 Warszawa, Poland

Received 2 April 1997, in final form 13 August 1997

Abstract. FeCrCuNbSiB nanocrystalline alloys, with low fractions of the crystalline phase (10–25%), have been studied by means of static magnetic measurements and Mössbauer spectroscopy over a wide temperature range (4.2–800 K). As a reference the temperature dependences of the hyperfine parameters measured in ordered Fe–Si alloys were used. It has been shown that at temperatures close to the Curie point of the amorphous matrix the coercivity exhibits a maximum that corresponds to a kink in the thermal evolution of the hyperfine field of the crystalline phase. These effects originate from the lessening of the interphase exchange interactions at the ferro–paramagnetic phase transition of the amorphous matrix and superparamagnetic fluctuations of the magnetization in single-domain grains. A mechanism considering different energy contributions as well as their changes with temperature in such a mesoscopic system is discussed.

1. Introduction

Magnetic granular materials have widely been investigated during recent years because of their fundamental scientific interest as well as potential applications. Among these materials nanocrystalline ferromagnets produced by a partial devitrification of Fe-based amorphous metallic alloys exhibit excellent soft magnetic properties [1–4]. The most prominent example of these alloys has the nominal composition $Fe_{73.5}CuNb_3Si_{13.5}B_9$ (trade name Finemet introduced by Hitachi Metals, Ltd) [1]. The nanocrystalline state is created by the controlled annealing of the as-cast amorphous ribbon above its crystallization temperature. After the heat treatment the material shows a homogeneous structure of α-FeSi ultrafine particles (with the average diameter 10–20 nm) embedded in a residual amorphous matrix. The special interest in the basic investigations of the materials considered arises from their magnetically two-phase structure with a wide spectrum of macroscopic magnetic properties. These properties are actually determined by the nature of each phase separately as well as by the interphase magnetic interactions. Since the Curie temperature of the amorphous matrix is much lower than that of the FeSi nanocrystals, depending on the temperature, the effect of the intergranular phase being either in ferromagnetic or paramagnetic state can be investigated, in both cases for the very same assembly of grains [5–8].

The kinetics of crystallization as well as the physical properties of nanocrystalline alloys obtained by the devitrification of their amorphous precursors have widely been investigated by means of different methods [1–9]. Among the experimental techniques, one which is superior to many others, owing to its local probe, is Mössbauer spectrometry, since Fe atoms, being in different chemical and electronic surroundings, give separate contributions to the

0953-8984/97/4710485+16$19.50

spectra, and these contributions can usually be separated from each other. Because of this Mössbauer spectrometry allows us to investigate the changes in Fe neighbourhoods during the annealing process and in FeCuNbSiB alloys revealed the presence of crystalline and amorphous phases [10, 11]. Although many Mössbauer studies of Finemet nanocrystalline materials give a qualitative agreement on the rate of crystallization and the nature of the crystalline phases, nevertheless, the detailed and accurate quantitative interpretation cannot be performed. The similar magnetic characteristics (e.g. values of hyperfine fields) of the grains and the amorphous matrix prevent also temperature dependent studies of the Finemet-type materials.

In order to avoid these problems we modify the nominal composition of the starting amorphous alloy by addition of chromium, which lowers the Curie temperature and shifts significantly the hyperfine field towards lower fields, thus allowing a temperature dependent study of crystalline and amorphous phases. On the grounds of static magnetization measurements it has been shown that $Fe_{66}Cr_8CuNb_3Si_{13}B_9$ nanocrystalline alloy with low volume fraction of the crystalline phase exhibits a superparamagnetic behaviour at elevated temperatures [5, 12]. The parameter characteristic of the superparamagnetic state is the blocking temperature defined as a temperature below which the superparamagnetic relaxation is negligible. It is known, however, that the blocking temperature is not uniquely defined but it is related to the time scale of the experimental technique applied. In the magnetization measurements presented in [5] and [12] the blocking temperature was estimated for a superparamagnetic relaxation time of the order of 10^2 s, whereas the Mössbauer spectroscopy allows us to define this temperature for the relaxation time of about 10^{-8}–10^{-9} s [13]. The aim of this paper is to get a microscopic insight into the dynamics of the magnetization processes involved by carrying out detailed Mössbauer studies over a wide temperature range on the as-quenched as well as heat-treated samples. The results obtained are related to the bulk magnetic properties measured by the conventional method at elevated temperatures.

2. Experimental details

An amorphous ribbon of the $Fe_{66}Cr_8CuNb_3Si_{13}B_9$ alloy (5 mm wide and 25 μm thick) was prepared by the single-roller melt-spinning technique. It has already been shown that annealing of such amorphous ribbon above its crystallization temperature results in creation of a nanocrystalline structure of α-FeSi grains of about 10 nm of diameter [5, 12]. In this work, in order to obtain the samples at different stages of crystallization, the as-quenched ribbons were isothermally annealed at 800 K under vacuum for 10, 20, 40 and 60 min. The magnetic behaviour of the created nanocrystalline samples was studied with a vibrating sample magnetometer and M–H loop tracer over a wide range of elevated temperatures whereas the magnetic properties in the microscale with Mössbauer spectroscopy. These experiments were performed in a transmission geometry using a conventional spectrometer with a constant acceleration signal and a ^{57}Co source diffused into a rhodium matrix. The samples, consisting of 4 cm^2 sheets of ribbon (in amorphous or nanocrystalline state) were placed under vacuum either in a bath cryostat or in a furnace, which enables measurements over the temperature range 4.2–800 K. Since the registration time of the Mössbauer spectra is long, the highest temperature applied to an individual sample was chosen so as to avoid any structural evolution within the amorphous–crystal transformation at the time of measurements (77 K Mössbauer spectra have systematically been registered after high-temperature experiments confirming that no further changes in structure occurred at the time of measurements). Most of the Mössbauer spectra were recorded with an unpolarized γ-beam oriented perpendicularly to the ribbon plane, whereas some others were obtained

under the magic angle in order to prevent the effects caused by the ferromagnetic domain texture.

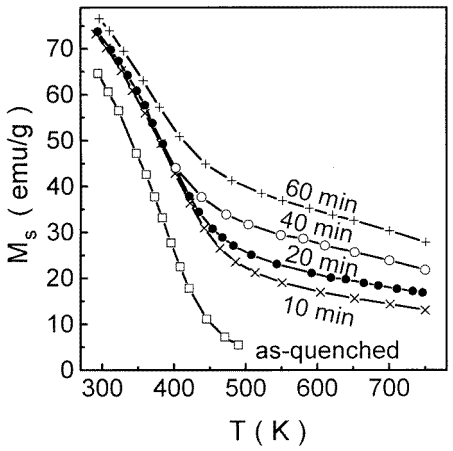

Figure 1. Temperature dependence of the saturation magnetization measured at 1.5 T of the as-quenched $Fe_{66}Cr_8CuNb_3Si_{13}B_9$ alloy and a series of samples annealed at 800 K.

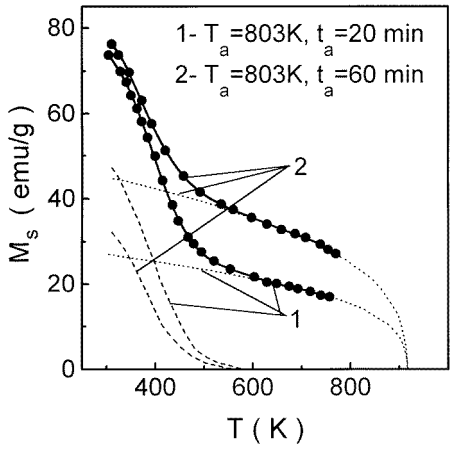

Figure 2. Saturation magnetization against temperature of selected nanocrystalline samples: experimental curve—solid line, crystalline phase contribution—dotted line, amorphous phase contribution—broken line.

3. Experimental results

3.1. Static magnetic measurements

The temperature dependences of the saturation magnetization measured in the field of 1.5 T on both as-quenched and annealed samples are shown in figure 1 and they reflect the evolution of the crystalline phase with the annealing time. In nanocrystalline samples the shape of the curves is typical of two-phase material in which both phases are ferromagnetic but with quite different Curie temperature (α-FeSi grains and residual amorphous matrix,

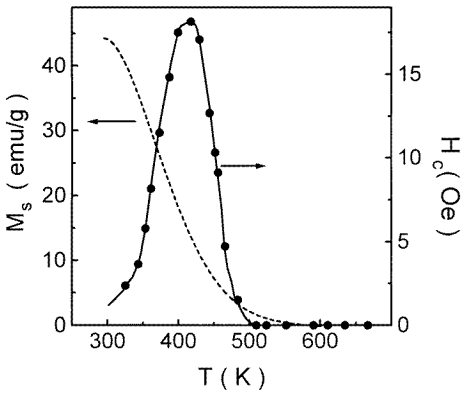

Figure 3. Correlation between the temperature dependence of the magnetization of the residual amorphous matrix and the coercivity in the sample annealed at 800 K for 20 min.

in the case considered). The saturation magnetization for such heterogeneous material can simply be considered as a weighted average of the magnetization of two independent phases—amorphous $M_{am}(T)$ and crystalline $M_{cr}(T)$:

$$M_s(T) = (1 - p)M_{am}(T) + pM_{cr}(T) \tag{1}$$

where p is the volume fraction of the crystalline phase. The temperature dependence of the individual phase (amorphous or crystalline) can be described by

$$M_s(T) = M_s(0)[1 - T/T_c]^{\beta} \tag{2}$$

where the exponent $\beta = 0.36$, as predicted for a Heisenberg ferromagnet, and $M_s(0)$ is the saturation magnetization at $T = 0$ K. Equation (1) holds whether the amorphous phase is ferromagnetic ($M_{am} > 0$) or paramagnetic ($M_{am} = 0$). Since for temperatures higher than the Curie point of the amorphous matrix only the nanocrystalline α-FeSi phase accounts for the observed magnetization, fitting of the experimental dependences to the above equations gives the contributions from separate phases; the results of the fitting procedure for selected samples are presented in figure 2. They allow us in turn to estimate the volume fraction of the crystalline phase p as well as Si content in the Fe–Si grains for each of the samples investigated [3, 5]. It has been found that the Curie temperature of the nanocrystalline phase is almost independent on the annealing time and it is about 645 °C which corresponds to the Si content of about 16%.

Figure 3 shows the temperature dependence of the coercivity as well as the contribution to the saturation magnetization originating from the amorphous phase in the sample annealed for 20 min. This sample exhibits nanocrystalline structure with $p \approx 15\%$ and grains of about 10 nm diameter [12]. At room temperature the sample behaves as a relatively good soft ferromagnet with low coercivity and high permeability. With the increase of temperature, but even at temperatures far below the Curie point of the amorphous matrix, a rapid degradation of the soft magnetic properties is observed and it is manifested by a sudden increase of the coercivity. The magnetic hardening of the material is caused by the decrease of the magnetization of the residual amorphous phase (see figure 3) which leads to a progressive magnetic decoupling of the grains. When the temperature reaches the Curie point of the amorphous phase, the grains become magnetically isolated (the distances between the grains are about 10 nm that is large enough to prevent interparticle interactions) and α-FeSi crystals form an assembly of non-interacting randomly oriented ferromagnetic

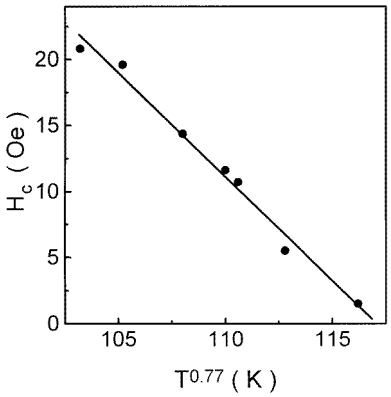

Figure 4. Coercivity as a function of $T^{0.77}$ for the sample annealed at 800 K for 20 min (zero coercivity is achieved at $T_B \approx 490$ K).

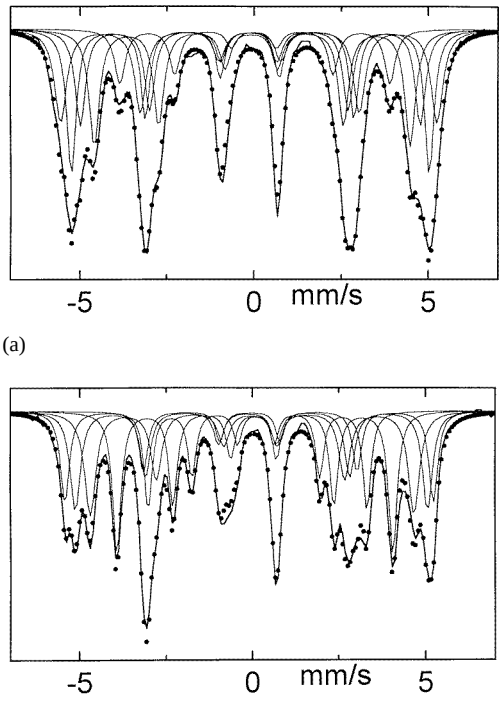

Figure 5. Mössbauer spectra of $Fe_{87.2}Si_{12.8}$ (a) and $Fe_{81.3}Si_{18.7}$ (b) ordered alloys.

single-domain particles. The temperature dependence of the coercivity for such assembly of grains is dominated by thermal fluctuations and it is given by [15]:

$$H_c = H_c(0)[1 - (T/T_B)^{0.77}] \tag{3}$$

where $H_c(0)$ is the coercivity at $T = 0$ K and T_B is the superparamagnetic blocking temperature. The $T^{0.77}$ dependence of the coercivity, for temperatures above the Curie point of the amorphous phase, is shown in figure 4 and confirms the expected linear behaviour

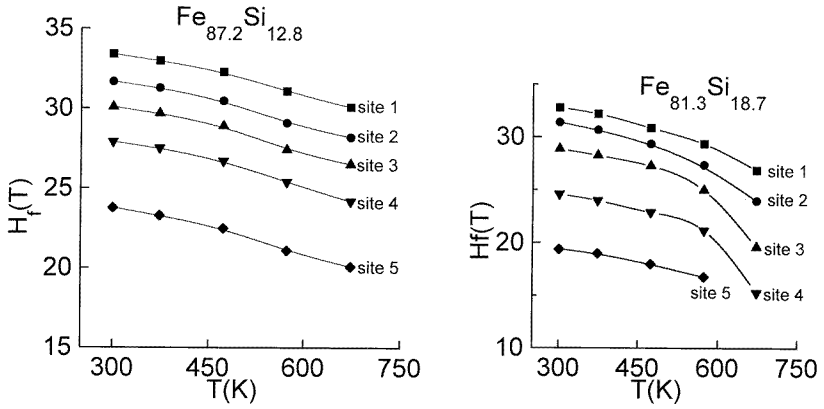

(a) (b)

Figure 6. Temperature dependence of the hyperfine fields for different Fe sites in $Fe_{87.2}Si_{12.8}$ (a) and $Fe_{81.3}Si_{18.7}$ (b) ordered alloys (the sites 1, 2, 3, 4 and 5 correspond to inequivalent configurations for Fe atoms which have 8, 7, 6, 5, and 4 iron near neighbours, respectively).

with the blocking temperature $T_B \approx 490$ K. At sufficiently high temperature (above T_B) the magnetic anisotropy energy barrier is overcome by the thermal energy and conventional magnetization measurements show the superparamagnetic behaviour of the α-FeSi grains, in agreement with previous observations [5].

3.2. Mössbauer spectrometry

The x-ray diffraction studies of the annealed FeCrCuNbSiB alloys show that the devitrification leads to the formation of Fe–Si crystalline phase with Si content of about 14% [12]. Although crystalline Fe–Si alloys have been investigated by Mössbauer spectroscopy [10, 16] there are no experimental results on the temperature evolution of hyperfine parameters in Fe–Si crystals. Since the knowledge of these data is essential in the correct interpretation of the results obtained in FeCrCuNbSiB nanocrystalline materials, the present studies have been extended over the Mössbauer investigations of Fe–Si alloys.

3.2.1. Ordered Fe–Si alloys. Systematic temperature dependent Mössbauer studies of some crystalline iron–silicon alloys (prepared by the method described in [16]) in the concentration range 5–26 at.% Si have been performed and the details will be published elsewhere [17]. Two representative spectra obtained for silicon content 12.8 and 18.7 at.% at room temperature are shown in figure 5. It has been found that up to 10%, silicon is soluble in bcc iron and Si atoms randomly substitute Fe atoms. In the concentration range 10–13%, the $B2$ crystalline structure, in which iron and silicon atoms randomly occupy the $[\frac{1}{2}, \frac{1}{2}, \frac{1}{2}]$ position in the cubic unit cell formed by iron atoms, is observed. A further increase of the silicon content (above 14 at.% Si) leads to the phase transition towards the ordered DO_3 structure, in agreement with previous study [10, 16]. The unit cell in the DO_3 crystal structure contains roughly eight unit cells of the α-Fe and consists of 16 atoms forming two cubic sub-lattices. One of them (denoted as A) contains eight Fe atoms, whereas the other (denoted as D) contains both Fe and Si atoms. Because of this many inequivalent Fe sites (each having various numbers of silicon nearest neighbours) exist in the crystal, and these different configurations can partially be resolved in the Mössbauer spectra. In the course of the fitting procedure it has been shown that five inequivalent configurations for Fe atoms

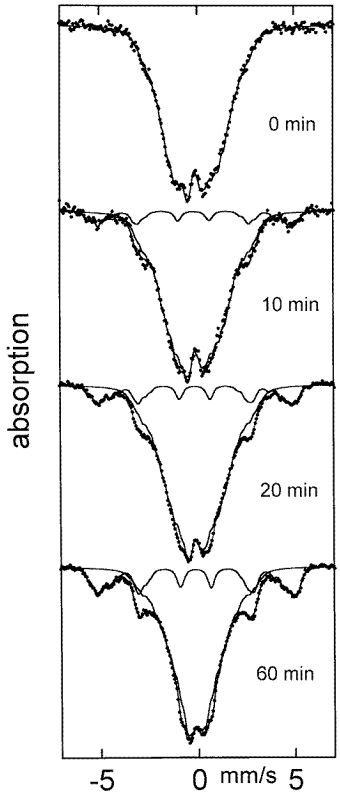

Figure 7. Room-temperature Mössbauer spectra of the as-quenched $Fe_{66}Cr_8CuNb_3Si_{13}B_9$ alloy and a series of samples annealed at 800 K for the annealing times indicated in the figure.

which have different numbers of iron near neighbours (from eight to four) can be resolved in the obtained Mössbauer spectra—in figure 6 they are described as the sites 1–5, respectively. The hyperfine parameters of different iron sites and their changes with temperature, shown for the selected samples in figure 6, have then been used as reference data in fitting of the spectra obtained in FeCrCuNbSiB nanocrystalline samples.

3.2.2. Crystallization behaviour of FeCrCuNbSiB alloy. The Mössbauer spectra of the $Fe_{66}Cr_8CuNb_3Si_{13}B_9$ in the as-quenched state and in the samples annealed at 800 K for various times recorded at room temperature are shown in figure 7. They reveal the transformation from the initial amorphous material with the spectrum consisting of a broad sextet characteristic of disordered amorphous structure to the nanocrystalline material containing two magnetic phases. The spectra of the annealed samples exhibit a complex hyperfine structure in which sharp lines originating from the crystalline phase are superimposed with the broad overlapping lines of the residual amorphous matrix. To prevent errors arising from the magnetic texture [18, 19] it has been checked that the effects of the domain structure can be neglected for both as-quenched and annealed samples. Consequently, the spectra were fitted assuming the free-texture behaviour of the amorphous contribution. The hyperfine parameters of the subspectra were obtained in the course of the fitting procedure under the assumption that the values of the isomer shift, the quadrupolar shift and the hyperfine field of the crystalline component are similar to those obtained at the same temperature for ordered Fe–Si alloys with a particular composition. The computer separation of the amorphous and crystalline contributions of the spectra obtained

is shown in figure 7, whereas the representative detailed fit of the five subspectra of the crystalline component for the sample annealed at 800 K for 20 min is shown in figure 8. The comparison of this contribution to the spectra obtained for ordered Fe–Si alloys (see figure 5) demonstrates that the hyperfine structure of the crystalline phase in FeCrCuNbSiB nanocrystalline material is very similar to that of ordered Fe–12.8 at.% Si. The exact analysis (based on the relative intensities of the crystalline subspectra, as described in [10] and [16]) shows that the silicon concentration within the grains is about 14% and hardly depends on the annealing time. The fraction of the crystalline phase in the samples studied was estimated in iron weight assuming the same value of the recoil-free fraction (Lamb–Mössbauer f-factor) for both crystalline and amorphous phases. The obtained dependence of the crystalline fraction on the annealing time is shown in figure 9 and compared to that deduced from the magnetization measurements. It is seen that both experimental methods give almost the same (within the experimental error) results and reveal the quasi-linear kinetics of the amorphous to crystalline transformation for the annealing times in the range 10–60 min.

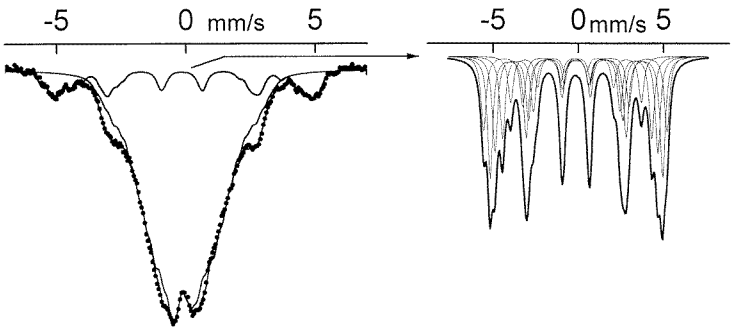

Figure 8. Room-temperature Mössbauer spectrum of the sample annealed for 20 min (left figure) and the decomposition of the crystalline phase component (represented by a solid line in the left figure) for five inequivalent Fe sites (right).

The distribution of the hyperfine field of the as-quenched ribbon shows a broad maximum which is typical of the amorphous state with a random distribution of the local environments whereas in the heat-treated samples a second peak appears in the high-field region attributed to the Fe–Si crystalline phase. The room-temperature average values of the hyperfine field of the amorphous and crystalline contributions are about 10 T and 30 T, respectively. The representative distributions of the hyperfine fields for the residual amorphous phase are shown in figure 10 and compared to that of the as-quenched state. It is seen that the mean value of the hyperfine field of the amorphous phase shifts towards lower fields with the increase of the annealing time suggesting the relative increase of the chromium content in the matrix, in agreement with the previous suggestions [14]. This conclusion is further supported by the fact that values of the isomer shift of the amorphous contribution decrease simultaneously with the decrease of the hyperfine field indicating that the total density of the s electrons at the iron nucleus increases whereas the density of d electrons decreases. Moreover, it has been found that though the intensity of the crystalline (high-field) peak in the hyperfine field distribution increases, nevertheless its position does not shift with the evolution of crystallization. All these experimental facts confirm that chromium does not enter the precipitated crystalline grains but remains in the amorphous matrix and indicate an atomic segregation during the crystallization process.

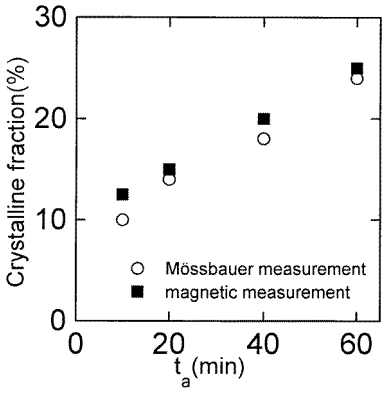

Figure 9. The volume fraction of the crystalline phase against the annealing time.

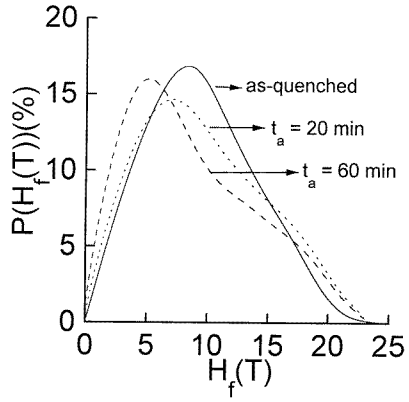

Figure 10. Distributions of the hyperfine fields of the amorphous phase in the as-quenched and two selected nanocrystalline samples at room temperature.

3.2.3. Temperature evolution of the Mössbauer spectra. Mössbauer measurements in the as-quenched and annealed samples have been performed over the temperature range 4.2–800 K. Figure 11 shows some representative spectra recorded at different temperatures in the nanocrystalline alloys obtained after annealing at 800 K for 20 min (figure 11(a)) and 60 min (figure 11(b)). The spectra change drastically their shape at around 400 K. Below that temperature they can be decomposed in two main magnetic components: one located in the low velocity range with broad and overlapping lines and a magnetic splitting which decreases as the temperature increases and another one, the outermost lines of which are well visible. Above 400 K the first component, attributed to the remaining amorphous phase, collapses to an asymmetric quadrupole doublet, whereas the second contribution, resulting from the crystalline precipitates, continues to display a magnetic hyperfine structure.

The spectra have been fitted assuming five inequivalent iron sites in Fe–Si grains with the temperature dependence of hyperfine parameters (isomer shift, quadrupolar shift and hyperfine field) similar to that obtained in crystalline FeSi alloys. Additionally, it has been taken into account that the populations of each iron site and the relative content of both amorphous and crystalline phases should be temperature independent. The series of Mössbauer spectra obtained at various temperatures for each of the samples were

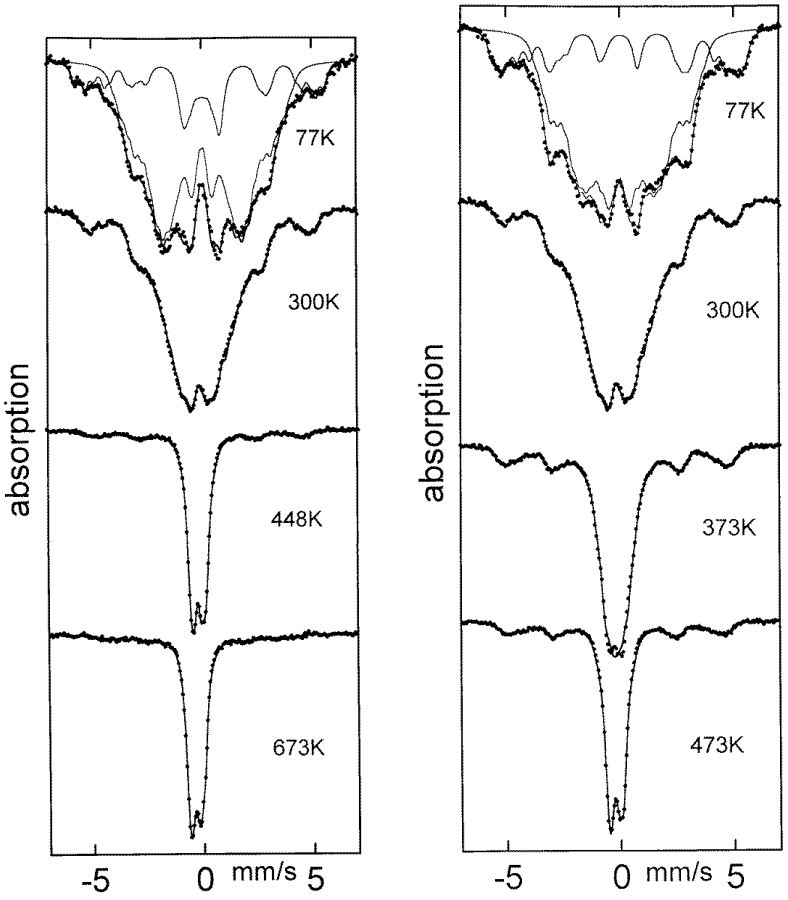

Figure 11. Temperature evolution of the Mössbauer spectra for the samples annealed at 800 K for 20 min (a) and 60 min (b).

successfully fitted in accordance with the above assumptions, except for the values of hyperfine parameters at high temperatures which were systematically smaller than those expected.

The mean values of the hyperfine field in the amorphous phase of the selected annealed samples are plotted as a function of temperature in figure 12. The fit of these results to (2) (shown as solid and broken lines in this figure) allows us to estimate the Curie temperature of the remaining amorphous phase. It is seen that T_c(am) decreases with the increase of crystalline fraction from 415 °C—i.e. the value which was found in the as-quenched sample—to 384 °C in the sample annealed for 60 min. However, the observed decrease of the Curie temperature is smaller than expected considering the increase of the Cr content in the residual amorphous matrix. It indicates that in the material with low crystalline fraction the ferromagnetically ordered crystallites can induce the ordering of Fe atoms in the matrix around the grains. These two competing mechanisms (enrichment in Cr atoms and induced magnetic ordering) can thus account for the observed only slight decrease of T_c(am). The role of the second mechanism leading to the Curie temperature enhancement is much better

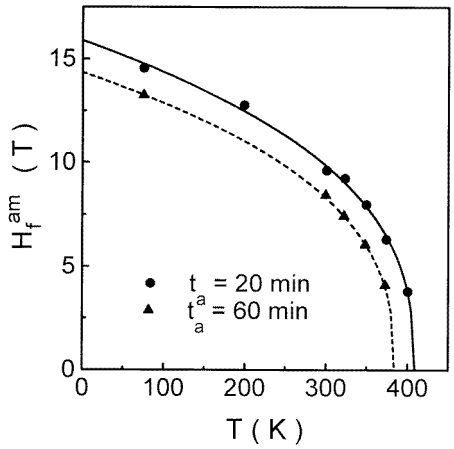

Figure 12. Temperature dependence of the average hyperfine field of the amorphous matrix for selected nanocrystalline samples (the annealing times are indicated in the figure).

visible in the material with high crystalline content, as reported in [8] and [20], due to strong intergrain interactions that propagate through the paramagnetic matrix.

The temperature dependences of mean values of the hyperfine field in the crystalline phase H_f^{cr} of the samples annealed for 20 and 60 min are shown in figure 13. For comparison the temperature evolution of the mean hyperfine field obtained in ordered Fe–12.8 at.% Si alloy is also presented in the same figure. It is seen that at elevated temperatures, for both of the heat-treated samples, the nanocrystalline phase exhibits a faster decrease in $H_f^{cr}(T)$ than in the ordered Fe–Si alloy and that this effect becomes more pronounced for lower crystalline fraction. Such a reduction of the hyperfine field may be attributed to the superparamagnetic behaviour of the nanocrystalline grains. The conventional magnetic measurements indicate that the sample annealed for 20 min exhibits superparamagnetic behaviour, with the relaxation time of the order of 10^2 s, at temperatures above $T_B = 490$ K (see section 3.1). For the Mössbauer spectrometry the superparamagnetic blocking temperature, defined as the temperature above which the superparamagnetic relaxation time is short compared to the time scale of the experiment (10^{-8}–10^{-9} s [13]), is obviously higher than 490 K. In practice, the sample always exhibits a distribution of the grain sizes, and consequently, a distribution of the blocking temperatures. Therefore, at a given temperature smaller particles may show superparamagnetic behaviour whereas others still exhibit magnetic ordering. But even below the blocking temperature, the magnetization vector may still fluctuate in the vicinity of the energy minimum (easy direction of magnetization). Since these collective magnetic excitations are fast compared to the time scale of Mössbauer spectroscopy, the observed magnetic splitting of the Mössbauer spectrum is proportional to the average value of the magnetic hyperfine field and hence smaller than it would be in the absence of superparamagnetic fluctuation effects. The reduction of the hyperfine field at elevated temperatures decreases with the increase of crystalline fraction (i.e. the annealing time) in the sample.

For both nanocrystalline samples it is clearly seen that the $H_f^{cr}(T)$ curve shows a distinctive change in curvature, which is observed in the form of a kink, at temperatures close to the Curie point of the amorphous matrix, confirming previous observations [14]. This anomaly is even better visible in the temperature evolution of hyperfine field in each

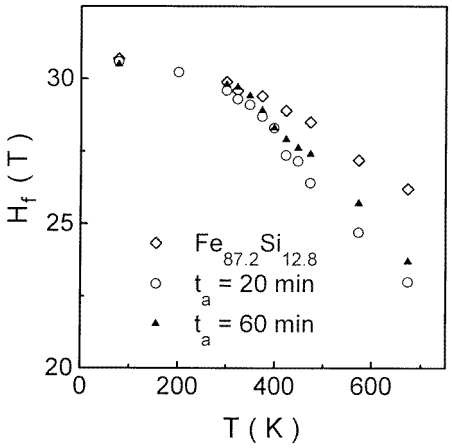

Figure 13. Temperature dependence of the mean hyperfine field of the crystalline phase of selected nanocrystalline samples and ordered $Fe_{87.2}Si_{12.8}$ alloy.

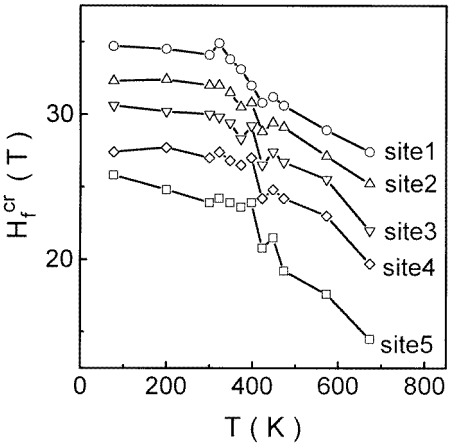

Figure 14. Temperature dependence of the hyperfine fields for different Fe sites in Fe–Si crystalline phase in $Fe_{66}Cr_8CuNb_3Si_{13}B_9$ sample annealed at 800 K for 20 min.

of the five components corresponding to different Fe sites in Fe–Si grains, as shown in figure 14. The results presented indicate that the intergranular matrix plays an important role in magnetic behaviour of the crystalline phase due to the interactions between the grains and the matrix.

4. Discussion

Thermal evolution of the magnetic parameters obtained by static magnetic measurements and by Mössbauer spectrometry shows characteristic deviations from the monotonic dependences, namely, the peak of the coercivity and the kink in the hyperfine field of the crystalline phase, both located at temperatures close to the Curie point of the residual amorphous phase. These experimental results indicate that there are two temperature

ranges in which the magnetic behaviour of the nanocrystalline material differs considerably: (i) a low-temperature region (below the Curie point of the amorphous matrix) with large saturation magnetization, low effective magnetostriction and reduced anisotropy in which both phases—crystalline and amorphous—are ferromagnetic, and (ii) an elevated-temperature region (above T_c(am)) in which the ferromagnetic grains are embedded in paramagnetic amorphous matrix. In this temperature range the properties of the material depend strongly on the volumetric fraction of the crystalline phase and, consequently, intergrain distances, which affect the type and the strength of the intergrain interactions.

The magnetic properties of these nanocrystalline materials and their temperature dependences can thus be described considering an assembly of single-domain particles distributed within a ferromagnetic or paramagnetic medium. Although in a real material there is a certain distribution in size and shape of the nanograins, for simplicity, to model the magnetic phenomena, the presence of identical particles is assumed. The basic energy terms contributing to the magnetic energy of an assembly of particles are:

(i) the magnetocrystalline anisotropy of a particle resulting from the spin–orbit coupling and related to the crystal symmetry, in the case of uniaxial anisotropy given by:

$$E(\theta) = KV \sin^2 \theta \tag{4}$$

where K is the magnetic anisotropy energy constant, V is the volume of the particle and θ is the angle between the easy axis of magnetization and the magnetization vector $\boldsymbol{M}$;

(ii) the shape anisotropy, for an ellipsoidal particle given by:

$$E_{sh} = \tfrac{1}{2} V(N_x M_x^2 + N_y M_y^2 + N_z M_z^2) \tag{5}$$

where $N_{x,y,z}$ are the demagnetizing factors;

(iii) the surface magnetic anisotropy which arises from the symmetry restriction at grain boundary and depends on the surface to volume ratio S/V, expressed by:

$$E_s = K_s(S/V) \cos^2 \psi \tag{6}$$

where K_s is the surface anisotropy constant and ψ is the angle between magnetization and normal to the grain surface;

(iv) the magnetoelastic anisotropy originating from the internal as well external stresses σ, due to magnetostrictive coupling given by:

$$E_\sigma = -\tfrac{3}{2} \lambda_s \sigma \cos^2 \theta \tag{7}$$

where λ_s is the saturation magnetostriction constant;

(v) the energy of the magnetic dipolar interactions between particles expressed by:

$$E_d = \boldsymbol{M}_1 \cdot \boldsymbol{M}_2 / r^3 - 3(\boldsymbol{M}_1 \cdot \boldsymbol{r})(\boldsymbol{M}_2 \cdot \boldsymbol{r})/r^5 \tag{8}$$

where $\boldsymbol{M}_i$ is the magnetization vector of the ith particle and r is the distance between the interacting particles;

(vi) the energy of the exchange interactions between the crystallite and the matrix (and/or another neighbouring crystal) given by:

$$E_{ex} = -K_{ex} \boldsymbol{M}_1 \cdot \boldsymbol{M}_m \tag{9}$$

where K_{ex} is the exchange anisotropy energy constant, $\boldsymbol{M}_1$ and $\boldsymbol{M}_m$ are the magnetization vectors of the grain and surrounding matrix, respectively;

(vii) the thermal energy which destabilizes the magnetic ordering and leads to the spontaneous fluctuation of magnetization inside the grain:

$$E_{th} = k_B T \tag{10}$$

where k_B is the Boltzmann constant.

In the case of non-interacting ultrafine single-domain particles, the thermal energy can overcome other energy contributions leading to the fluctuations of magnetization among easy directions, i.e. to a superparamagnetic state with the relaxation time τ given by the Néel theory [21]:

$$\tau = \tau_0 \exp(KV/k_BT). \tag{11}$$

On the basis of these different energy contributions, the interpretation of the thermal changes of the magnetic properties in the nanocrystalline materials can be proposed. At low temperatures the short-range exchange interactions between the crystalline grains and the amorphous matrix (9) are dominant. They result in reduction of the magnetocrystalline anisotropy term (4) and negligible contribution from shape (5), dipolar interactions (8) and surface (6) energy terms. The magnetoelastic contribution (7), due to a small effective magnetostriction constant (resulting from a negative contribution of the crystalline phase and positive one of the amorphous matrix [3]), can also be neglected. Such mechanisms provide the basis for good soft magnetic properties. In material with low volume fraction of the crystalline phase, like in the alloys considered in this paper, the increase of the temperature causes the fast decrease of the magnetization of the amorphous matrix, and, consequently, the decrease of the exchange interaction between the grains and the matrix (9), leading to magnetic decoupling of the α FeSi nanocrystals. This is the most important energy term that affects the behaviour of the sample. The lack of the exchange coupling means in turn that within each of the grains the magnetization follows the local easy axis increasing of the magnetocrystalline (4), shape (5) and surface (6) anisotropy energy contributions. Because of this a fast degradation of the soft magnetic properties is observed and it is evidenced by the increase of coercivity (see figure 3). For such assembly of non-interacting single-domain particles, with further increase of the temperature, the thermal energy (10) destabilizes the magnetic state and the coercivity decreases, according to (2). Finally, at sufficiently high temperatures thermal fluctuations tend to overcome the magnetic anisotropy energy barrier and the magnetic behaviour of the material is dominated by the superparamagnetic relaxation. The peculiar behaviour of the hyperfine field of the crystalline phase, which is manifested in the form of a kink in its temperature dependence (corresponding to the maximum of the coercivity), can thus be understood in terms of a sudden change of the magnetic energy contributions at temperatures close to the Curie point of the amorphous matrix. The change of the magnetic energy in the system close to T_c(am), which can largely be ascribed to the loss of the exchange interactions between the crystalline and amorphous phases, can roughly be estimated in the mean-field model [22, 23] from the difference of the transition temperatures in the materials with and without exchange coupling, as shown in figure 15 for the selected sample. The nanocrystalline system with the exchange interactions between crystalline and amorphous phases (low-temperature region for the nanocrystalline sample which corresponds to the temperature dependence of the hyperfine field of Fe–Si ordered alloy) fits to the dashed curve, whereas that of the magnetically isolated Fe–Si grains (high-temperature region for the nanocrystalline sample) to the full curve. It is seen that the difference in the magnetic transition temperatures is about 190 K which corresponds to 2.6×10^{-21} J.

Moreover, in the low-temperature region the $H_f^{cr}(T)$ curves obtained for different samples are superimposed whereas at elevated temperatures a variation of the $H_f^{cr}(T)$ for the sample annealed for longer time is slower than for the sample with lower fraction of the crystalline phase (see figure 13). Since the composition of the grains does not change with the annealing time, two mechanisms may be responsible for the differences observed with the increase of the annealing time: (i) the increase of the grain sizes and (ii) the increase of the

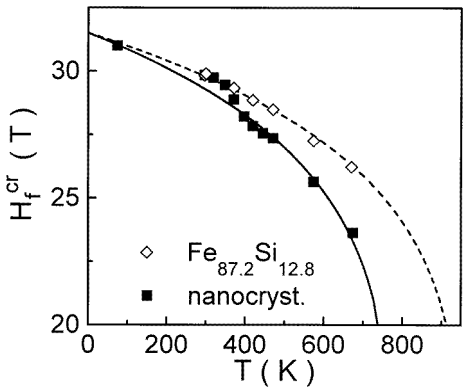

Figure 15. Variation of the average hyperfine field of the crystalline phase in the nanocrystalline sample annealed for 20 min and in $Fe_{87.2}Si_{12.8}$ ordered alloy with temperature; the lines represent the fit of the data to the mean-field model.

crystalline fraction and thus the decrease of the intergrain distances which, below a certain value, can lead to the occurrence of the long-range magnetic dipolar interactions between the grains increasing the magnetic energy barrier and suppressing thermal fluctuations.

In contrast, in the alloys with high crystalline fraction (70–80%, as typical in soft magnetic nanocrystalline alloys [6–8, 24]) the distances between the grains are about 1–2 nm and the intergranular interactions (of long-range dipolar (8) and short-range exchange (9) origin) occur at elevated temperatures through the paramagnetic amorphous matrix [6, 7]. In this case only slow increase of the coercivity and thus the slow deterioration of the soft magnetic properties is observed at temperatures well above the Curie point of the intergranular amorphous phase [8, 24]. Moreover, the temperature evolution of hyperfine field of the crystalline phase is smooth, without any indication of the presence of a kink at the ferro–paramagnetic phase transition of the amorphous matrix [25]. This behaviour reflects the slow progressive decrease of the intergrain coupling. The interactions lead to ordering of magnetic moments and prevent superparamagnetic relaxation even at elevated temperatures. It can be expected that the paramagnetic matrix plays in this case an important role as a medium transmitting these interactions [26].

5. Conclusions

Conventional magnetic measurements and Mössbauer spectroscopy investigations of $Fe_{66}Cr_8CuNb_3Si_{13}B_9$ nanocrystalline alloys at different stages of crystallization have been performed over a wide range of temperatures. It has been shown that during annealing atomic segregation occurs within the amorphous material leading to the formation of Fe–Si nanocrystals and Cr-rich amorphous matrix. The behaviour of the crystalline phase was approximated by the ordered Fe–Si alloys. Because of this detailed temperature dependent studies of the ordered Fe–Si alloys have been performed and the results obtained were used as reference data for the crystalline phase in nanocrystalline FeCrCuNbSiB alloys. The volume fraction of the crystalline phase estimated from the bulk magnetization measurements corresponds well to that obtained from the Mössbauer spectroscopy.

Nanocrystalline material composed of single-domain ferromagnetic particles embedded in the amorphous matrix and well separated one from each other shows peculiar behaviour

in the temperature evolutions of magnetic parameters. It is manifested in the form of a peak in the coercivity and the corresponding kink in the hyperfine field of the crystalline phase, both at temperatures close to the Curie point of the amorphous matrix. Analysis of the total energy of such a system reveals that at low temperatures the exchange interactions between the crystalline and amorphous phases lead to the collective magnetic behaviour of the material whereas the ferro–paramagnetic phase transition of the amorphous matrix results in a magnetic decoupling of the grains. The lessening of the exchange energy, which in the materials studied was estimated to correspond to thermal energy of about 190 K, is particularly responsible for the observed distortion of the $H_f^{cr}(T)$ dependence from the expected one represented by the curve obtained for ordered Fe–Si alloys. Decoupling of the grains leads in turn to the increase of the effective anisotropy of the individual crystallites and enhances the coercivity. At elevated temperatures the behaviour of the assembly of grains embedded in the paramagnetic matrix depends mainly on the intergrain distances. In the samples with the lowest crystalline fraction (10–15%) the thermal energy causes superparamagnetic fluctuations of the magnetization vectors in single-domain grains. With the increase of the crystallite contents and corresponding decrease of the intergrain distances down to 5–6 nm, the dipolar interactions between the grains increase the energy barrier and suppress superparamagnetic fluctuations.

References

[1] Yoshizawa Y, Oguma S and Yamauchi K 1988 *J. Appl. Phys.* **64** 6044
[2] Yoshizawa Y and Yamauchi K 1990 *Mater. Trans. JIM* **31** 307
[3] Herzer G 1992 *IEEE Trans. Magn.* **MAG-26** 1397
[4] Herzer G 1993 *Phys. Scr.* T **49** 307
[5] Ślawska-Waniewska A, Gutowski M, Lachowicz H K, Kulik T and Matyja H 1992 *Phys. Rev.* B **46** 14 594
[6] Ślawska-Waniewska A, Kuźmiński M, Gutowski M and Lachowicz H K 1993 *IEEE Trans. Magn.* **29** 2628
[7] Lachowicz H K and Ślawska-Waniewska A 1994 *J. Magn. Magn. Mater.* **133** 238
[8] Hernando A and Kulik T 1994 *Phys. Rev.* B **49** 7064
[9] Hono K, Zhang Y, Inoue A and Sakurai T 1995 *Mater.Trans. JIM* **7** 909
[10] Rixecker G, Schaaf P and Gonser U 1992 *J. Phys.: Condens. Matter* **4** 10 295
[11] Pradell T, Clavaguera N, Zhu Jie and Clavaguera-Mora M T 1995 *J. Phys.: Condens. Matter* **7** 4129
Hampel G, Pundt A and Hesse J 1992 *J. Phys.: Condens. Matter* **4** 3195
Goria P, Garitaonandia J S and Barandiaran J M 1996 *J. Phys.: Condens. Matter* **8** 5925
[12] Ślawska-Waniewska A, Gutowski M, Kuźmiński M, Dynowska E and Lachowicz H K 1994 *Nanophase Materials* ed G C Hadjipanayis and R W Siegel (Deventer: Kluwer) p 721
[13] Morup S 1983 *J. Magn. Magn. Mater.* **37** 39
[14] Jędryka E, Randrianantoandro N, Greneche J M, Ślawska-Waniewska A and Lachowicz H K 1995 *J. Magn. Magn. Mater.* **140–144** 451
[15] Pfeifer H 1990 *Phys. Status Solidi* a **118** 295
[16] Rixecker G, Schaaf P and Gonser U 1993 *Phys. Status Solidi* a **139** 309 references therein
[17] Randrianantoandro N, Gaffet E and Greneche J M 1997 to be published
[18] Greneche J M and Varret F 1982 *J. Phys. C: Solid State Phys.* **15** 5333
[19] Greneche J M and Varret F 1982 *J. Physique Lett.* **43** L233
[20] Hernando A and Navarro I and Gorria P 1995 *Phys. Rev.* B **51** 3281
[21] Néel L 1949 *Ann. Geophys.* **5** 99
[22] Morup S and Christensen H 1987 *J. Magn. Magn. Mater.* **68** 160
[23] Morup S 1992 *Studies of Magnetic Properties of Fine Particles and their Relevance to Materials Science* ed J L Dormann and D Fiorani (Amsterdam: Elsevier) p 125
[24] Ślawska-Waniewska A, Nowicki P, Lachowicz H K, Gorria P, Barandiaran J M and Hernando A 1994 *Phys. Rev.* B **50** 5465
[25] Greneche J M and Ślawska-Waniewska A 1997 *Mater. Sci. Eng.* A **526** 226–8
[26] Navarro I, Ortuno M and Hernando A 1996 *Phys. Rev.* B **53** 11 656